Knudsen forces on microcantilevers

A. Passian[a] and A. Wig
Oak Ridge National Laboratory, Bethel Valley Road, Oak Ridge, Tennessee 37830

F. Meriaudeau
Université de Bourgogne, IUT du Creusot, Le2i, 12 rue de la Fonderie, 71200 Le Creusot, France

T. L. Ferrell and T. Thundat
Oak Ridge National Laboratory, Bethel Valley Road, Oak Ridge, Tennessee 37830

(Received 21 March 2002; accepted 23 August 2002)

When two surfaces at two different temperatures are separated by a distance comparable to a mean-free path of the molecules of the ambient medium, the surfaces experience Knudsen force. This mechanical force can be important in microelectromechanical systems and in atomic force microscopy. A theoretical discussion of the magnitude of the forces and the conditions where they can be encountered is discussed. A potential application of the Knudsen force in designing a cantilever-based vacuum gauge is discussed. © *2002 American Institute of Physics.*
[DOI: 10.1063/1.1515108]

I. INTRODUCTION

Knudsen forces are mechanical forces that exist between two surfaces at two different temperatures separated by a distance of one or a fraction of a mean-free path of the molecules of the medium. Though Knudsen forces are extremely small in most cases involving microcantilevers, there exist situations where these forces can be large.

Microcantilevers are routinely used in atomic force microscopy (AFM). In AFM, microcantilevers are brought in close proximity to a surface to be imaged. The distance between the cantilever and the sample surface is equal to the probing tip at the free end of the cantilever. This separation is many microns in most cases: Much higher than the mean-free path of the molecules in air at normal pressure. However, AFM can also be used in a vacuum where the mean-free path is larger than the distance of separation between the cantilever and the sample surfaces. In most cases, there exists a temperature difference between the cantilever and the surface. This temperature difference can originate from many different sources. For example, a piezoresistive cantilever is always at a higher temperature due to resistive heating of the cantilever. Even in the commonly used optical beam deflection technique, the cantilever is at a higher temperature due to laser heating of the surface. If the cantilever and the sample surfaces have different optical absorption, that can lead to a temperature difference between the cantilever and the sample surface. Thus, the two necessary conditions required for Knudsen forces namely temperature difference and separation distances comparable to mean-free path length of the molecules in the immersed medium are often encountered in many cases.

There are several scenarios where Knudsen forces play a role in microelectromechanical systems structures, for example, sensors based on microcantilevers. Recently, many physical, chemical, and biological sensors are demonstrated using microcantilevers. Though Knudsen forces will be small in most cases involving microcantilever sensors, there exist a few cases where Knudsen forces can be large. For example, when the capacitive detection method is used to monitor microcantilever motion in low-pressure conditions. One example will be detecting infrared radiation using bimaterial microcantilevers using capacitive monitoring of cantilever motion. To improve the thermal sensitivity of the system, it can be evacuated to low pressures to decrease the loss of heat energy from the cantilever. Knudsen forces can be important in low-pressure vacuum AFM where the sample is heated. In this case, there exists a Knudsen force between cantilever and the sample. Another example will be a piezoresistive cantilever imaging an object at room temperature in a vacuum.

II. BACKGROUND THEORY

One of the ways through which a gas in a vacuum system can possess nonuniform density and pressure is the existence of temperature gradients in the gas or on the confining surfaces of the vessel.[1,2] In order to study the effect of such thermally induced nonuniformities, we consider a closed system containing a gas of a certain low pressure in equilibrium. The phenomenon of thermal transpiration[3–5] takes place in such a system if we, through some mechanism, maintain two different temperatures T_1 and T_2 in two different interior regions of the system, and if, as a result of this difference, a gas transport or a flow region is established so that a pressure variation from P_1 to P_2 is developed there. Knudsen[6] showed that the following relation holds under the steady-state conditions of the gas at low pressures, that is when the thermally induced flow and the pressure flow are in balance

$$\frac{P_1}{P_2} = \sqrt{\frac{T_1}{T_2}}. \tag{1}$$

[a]Author to whom all correspondence should be addressed; electronic mail: passian@utk.edu

Experimental and theoretical work have indicated deviations from this relation[2,7,8] and much work has been conducted to improve the accuracy of Eq. (1). Two geometries are of particular importance; cylindrical and planar.

Thermal transpiration systems composed of two concentric cylinders where a temperature gradient along or between the cylindrical surfaces gives rise to a pressure gradient which in turn results in transverse and longitudinal force densities in the flow field have been studied in conjunction with precise microbalance experiments.[9–12] Liang[13–16] worked an empirical equation for the pressure ratio in Eq. (1) based partially on experimental observations. Takaishi and Sensui[17] similarly gave an improved version of Liang's equation. Recently, these results were used to study the thermal transpiration in helium and nitrogen across an individual[18] or an array of silica capillaries.[19] Some related experimental,[20] theoretical [Bhatnagar-Gross-Krook (BGK) model],[21–26] and numerical [one-dimensional and two-dimensional direct simulation Monte Carlo (DSMC)][23,27–30] work can be mentioned in this regard. The Knudsen forces arising in such cases display a peak as a function of the Knudsen number.[12] The Knudsen number at temperature T and pressure P for a medium with viscosity η composed of molecules of mass M_m and mean-free-path λ can be defined for structures with a characteristic dimension d via[3]

$$\mathrm{Kn}=\frac{\lambda}{d}=\frac{\eta}{Pd}\sqrt{\frac{\pi R_0 T}{2M_m}}, \tag{2}$$

where the universal gas constant R_0 is related to the Boltzmann constant and the Avogadro's number by $R_0=kN_A$. Using this definition, the force is small in the low (near-continuum limit) and high (free molecular limit) Knudsen number regions, and exhibits a maximum in the transition region, i.e., the pressure region where both molecule–molecule and molecule–surface collisions are important in a transport process.

In the planar thermal transpiration systems, typically a flow field is set up around and near the surface of a single flat structure or between several planar structures as a result of the generation of a temperature gradient and its accompanied pressure gradient, for example, in conjunction with thermophoresis and radiometer effects.[5] The former is the the motion of a small particle in a region of the gas where a temperature gradient exists; for example, a flat or spherical particle inside a tube that has a varying temperature along its surface.[31] Similarly, the latter is the phenomenon responsible for the rotation of the vane of a Crookes radiometer upon exposure of the vane to light and thus generation of a temperature gradient in the direction from the exposed side of the vane to the unexposed side.[32,33] This type of energy transport between surfaces at different temperatures leads to the molecular radiometer force which is the basis of the Knudsen gauge, which is an absolute pressure gauge,[34–36] and the Knudsen compressor.[37] In an attempt to theoretically study such effects, the extent to which energy transfer takes place when a gas molecule strikes a surface is expressed in terms of the accommodation coefficient introduced by Knudsen.[6,5]

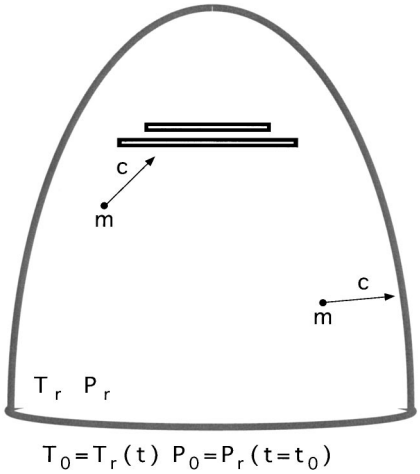

FIG. 1. Thermal transpiration system. The molecules of the confined gas moving in random directions collide predominantly with the surfaces of the vessel and the internal structures.

In the low Knudsen number regimes, the aforementioned flow fields are associated with a creeping motion of the gas (thermal creep or thermal slip) in a thin layer adjacent to the surface.[20,3] Thus, the molecules moving with a creep velocity transfer momentum in the flow field as a result of the presence of a temperature gradient. In this work, we will consider, in the high Knudsen number regime, the general form of the force between a microcantilever modeled as a planar object in close proximity to a sample/substrate also modeled as a flat surface. The cantilever is free to deflect under the Knudsen force but otherwise assumed to be stationary, that is any thermal undulations in the microcantilever are assumed to be negligible. The sample/substrate is assumed to be rigidly fixed. Furthermore, the degree of participation of the cantilever and substrate in heat conduction will be expressed in terms of two accommodation coefficients for the top and bottom surfaces of the cantilever, respectively, and a third for the substrate surface. There are currently sensing and imaging applications that require one side of the cantilever be coated, and thus the assumption of two different accommodation coefficients for the two sides of the cantilever is justified.

We now more specifically consider a simple vacuum system composed of a vessel and a pump as shown in Fig. 1. The pump is turned on at $t=t_0$ and operates continuously for $t>t_0$ until the desired mean-free-path λ is achieved. The initial ($t\leqslant t_0$) pressure, temperature, and mean-free path of the confined gas are $P(t_0)=P_0$, $T(t_0)=T_0$, and $\lambda(t_0)=\lambda_0$ where P_0 and T_0 are the atmospheric pressure and room temperature, respectively. For $t>t_0$, these quantities are denoted by $P(t)=P_r$, $T(t)=T_r$, and $\lambda(t)=\lambda_r$. The vessel is in thermal and mechanical equilibrium with the surrounding environment, that is the temperature on the vessel surfaces is uniform and equals T_0 and remains constant at all time t. At $t=t_0$, the number of molecules per unit volume of the gas n is of such high magnitudes that molecule–molecule, as opposed to molecule–surface, encounters dominate the kinetic properties of the gas. For example, for air at room temperature $T_0=20\,^{\circ}\mathrm{C}\,(=293.15\,\mathrm{K})$ with pressure P, and character-

istic length d expressed in units of μbar and μm, respectively, the Knudsen number Eq. (2) can be evaluated by[3]

$$\mathrm{Kn}=\frac{6.6\times 10^4}{Pd}, \tag{3}$$

which for $d=1\ \mu$m (a typical working distance in AFM studies) and for atmospheric pressure $P_0=1$ atm $=1013.25$ mbar yields $\mathrm{Kn}=0.065$ corresponding to $\lambda_0=65.1$ nm. Under these conditions, the gas can be considered as a fluid. When the pumping starts at $t=t_0$, an anisotropy in the velocity distribution of the gas molecules with a subsequent creation of various flow regimes are established. As the pumping progresses, the number density of the gas decreases due to the continuous removal of the molecules by the pump and thus the mean-free path increases reducing the dominance of the intermolecular collisions over the molecule–surface collisions. For fixed vessel dimensions, we thus enter a pressure regime where the frequency of molecule–surface collisions is of the same or higher order of magnitude as that of the intermolecular collisions.

For example, for a typical pressure of $P_r=20\ \mu$bar achieved by a mechanical pump, and a separation distance of $d=40\ \mu$m, Eq. (2) gives $\mathrm{Kn}=82.5$, that is the free molecular regime. This corresponds to a mean-free path of $\lambda_r=3300\ \mu\mathrm{m}\gg d$ appropriate for a Knudsen gas.

At such high Knudsen number regime, the pump is turned off whereafter the velocity distribution of the molecules will reach an isotropic steady state. No sources or sinks of gas are present at this stage. The microscopic properties of the resulting stationary gas can now be described by the Maxwell–Boltzmann distribution function which is the solution of the Boltzmann equation in the absence of intermolecular collisions. No temperature or pressure gradients exist in the system under these conditions. Denoting the molecular velocities by **c** and coordinates by **x** for a gas under the influence of the external force **F** the general form of Boltzmann equation is[23]

$$\frac{\partial f(\mathbf{x},\ \mathbf{c},\ t)}{\partial t}+\mathbf{c}\cdot\nabla_{\mathrm{c}} f(\boldsymbol{x},\ \boldsymbol{c},\ t)+\mathbf{F}\cdot\nabla_{\mathrm{x}} f(\mathbf{x},\ \mathbf{c},\ t)=Q(f,\ f), \tag{4}$$

where $Q(f,\ f)$ is the collision term and expresses the variation of f due to intermolecular collisions. Under certain assumptions regarding the function Q, it can be shown[23] that a Maxwellian distribution is the solution of $Q=0$ for a uniform steady state. Neglecting the influence of external forces on the confined gas such as gravity, for a local Maxwellian distribution, i.e., the solution to

$$Q(f,\ f)=\frac{\partial f(\mathbf{x},\ \mathbf{c},\ t)}{\partial t}+\mathbf{c}\cdot\nabla_{\mathrm{c}} f(\mathbf{x},\ \mathbf{c},\ t)=0, \tag{5}$$

f can be expressed at location $x=(x,\ y,\ z)$ and at the solid angle $d\Omega=\sin\theta d\theta d\varphi$ (see Fig. 2) as

$$f_\Omega(\mathbf{x},\ c)=\left(\frac{1}{2\pi RT_\Omega}\right)^{\frac{3}{2}}\exp\left(-\frac{c^2}{2RT_\Omega}\right), \tag{6}$$

where R is the gas constant, and T_Ω is the temperature of the molecules in the direction specified by the solid angle $d\Omega$ in the velocity phase space V_c at $\boldsymbol{x}$.[23] Wu[8] showed by comparing this solution Eq. (6) with another formal solution of Eq. (5) using a surface collision density function as the initial condition in a diffuse reflection boundary condition that the product of the square root of the directional temperature T_Ω, and the number density at $d\Omega$ denoted by n_Ω is a constant K throughout a gas described by f, that is $K=n_\Omega\sqrt{T_\Omega}$ is an invariant.

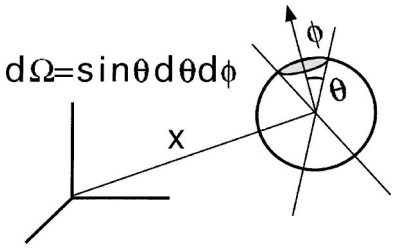

FIG. 2. The solid angle at the location **x**.

Returning to our discussion, if we now introduce a convex object, such as a microcantilever into the vacuum system described by Eq. (6), and assume that it is in thermal equilibrium with the Knudsen gas there, then the molecules colliding with the surface of the cantilever will transfer momentum to it in such a way that the net momentum of the microcantilever is zero. If we now increase the temperature of the cantilever to $T_c>T_r$ by some external means such as Joule heating or optically via irradiance by a laser beam, the local equilibrium is perturbed and a flow field is set up in the neighborhood of the cantilever. The velocity distribution of the molecules in this region will no longer be a Maxwellian due to the loss of the isotropicity. As mentioned in the Sec. I, the vacuum system is now called a thermal transpiration system and the kinetic energy transfer (thermal conduction) between the cantilever and the gas can be studied in terms of the ability of the surface material of the cantilever to alter the energy of an incident molecule upon a molecule–surface encounter. This can be formulated in terms of the coefficient of accommodation a which can be written for energy, temperature, or momentum and can have normal or tangential components. For example, when $a=1$, the incident molecule is reflected diffusely after complete accommodation to the surface temperature, whereas in the case $a=0$, the reflection is completely specular, and the temperature of the reflected molecule equals that of the incident. Obviously, in the absence of any directional preferences for the molecules distributed far from the cantilever, the net momentum transferred to the cantilever will again be zero if the accommodation coefficient is equal on both sides of the cantilever. These considerations are evident from Knudsen's radiometric pressure difference derived for a vane in a free molecular (collision-free) regime[6] which with our notations is given by

$$\Delta P=\frac{P_r}{2}\left[\sqrt{1+a_{cb}\tau}-\sqrt{1+a_{ct}\tau}\right], \tag{7}$$

where τ is the relative temperature, i.e., $\tau=T_c/T_r-1$. Knudsen showed by balancing the flow of molecules in a tube to zero that the quantity $PT^{-1/2}$ is a thermal transpiration in-

variant from which Eq. (1) is easily derived. However, Wu[8] showed that the departure from an isotropic distributions modifies this invariance, and introduced a function $I(\mathbf{x})$ as a measure of this departure. Thus, the new invariance for a Knudsen gas confined in a volume V was shown to be given by[8]

$$K = n_\Omega \sqrt{T_\Omega} = n(\mathbf{x}) \sqrt{T(\mathbf{x})} I(\mathbf{x}) = \frac{\gamma P(\mathbf{x}) I(\mathbf{x})}{\sqrt{T(\mathbf{x})}},$$

$$\text{for all } \mathbf{x} \in V, \tag{8}$$

where γ is a gas specific constant. Here, following Wu's results,[8] we will utilize this new invariance to derive a general expression for the force per unit area of the microcantilever. This can be accomplished by using Eq. (8) to calculate the pressure around the cantilever. We thus need to calculate the functions $T(\mathbf{x})$ and $I(\mathbf{x})$ in Eq. (8). We first note that since the molecules of mass m in the residual gas of density ρ move randomly and, therefore, the average of the square of the velocity $\langle c^2 \rangle = 3\langle c_z^2 \rangle$ we get the scalar pressure $P = \frac{1}{3}\rho\langle c^2 \rangle$, and from $\frac{1}{2}m\langle c^2 \rangle = \frac{3}{2}kT$ and $k = mR$ we get $P = \rho RT$. Then using the distribution function Eq. (6) and the invariance (8) the temperature at a point x in the gas $T = 1/3R\langle c^2 \rangle$ can be calculated by averaging the contributions to c^2 from all directions at the solid angle $d\Omega$ in the differential volume of the velocity phase space dV_c

$$3RT(\mathbf{x}) = \frac{\iiint_{V_c} c^2 n_\Omega f_\Omega(\mathbf{x}, c) dV_c}{\iiint_{V_c} n_\Omega f_\Omega(\mathbf{x}, c) dV_c}, \tag{9}$$

where $dV_c = c^2 dc d\Omega$ with $d\Omega = \sin\theta d\theta d\varphi$ at $\mathbf{c} = c(\sin\theta\sin\varphi, \sin\theta\cos\varphi, \cos\theta)$ in the spherical coordinates. The denominator in Eq. (9) is the number of the molecules per unit volume at $\mathbf{x}$

$$n(\mathbf{x}) = \int\int\int_{V_c} n_\Omega f_\Omega(\mathbf{x}, c) dV_c, \tag{10}$$

whereas the total number of molecules in the volume $V = \iiint_{V_x} dV_x$ of the system is

$$n = \int\int\int_{V_x} n(\mathbf{x})\, dV_x, \tag{11}$$

where $dV_x = dxdydz$ is a differential volume at $\mathbf{x} = (x, y, z)$ in Cartesian coordinates. Therefore,

$$\int\int\int_{V_c} n_\Omega f_\Omega(\mathbf{x}, c) dV_c = K \int\int\int_{V_c} \frac{f_\Omega(\mathbf{x}, c)}{\sqrt{T_\Omega}} dV_c, \tag{12}$$

or using Eqs. (10) and (6)

$$n(\mathbf{x}) = K\left(\frac{1}{2\pi R}\right)^{\frac{3}{2}} \int\int_\Omega T_\Omega^{-2} \left[\int_0^\infty c^2 \exp\left(-\frac{c^2}{2RT_\Omega} \right) dc \right] d\Omega$$

$$= \frac{K}{4\pi} \int\int_\Omega \frac{1}{\sqrt{T_\Omega}} d\Omega. \tag{13}$$

Similarly, the numerator of Eq. (9) can be written as

$$K \int\int\int_{V_c} \frac{c^2 f_\Omega(\mathrm{x}, c)}{\sqrt{T_\Omega}} dV_c, \tag{14}$$

which using the integrals (A1) and (A2) in the appendix can be written as

$$K\left(\frac{1}{2\pi R}\right)^{\frac{3}{2}} \int\int_\Omega T_\Omega^{-2} \left[\int_0^\infty c^4 \exp\left(-\frac{c^2}{2RT_\Omega} \right) dc \right] d\Omega$$

$$= \frac{3KR}{4\pi} \int\int_\Omega \sqrt{T_\Omega} d\Omega, \tag{15}$$

and thus $T(\mathbf{x})$ in Eq. (9) is given by

$$T(\mathbf{x}) = \frac{\int\int_\Omega T_\Omega^{1/2} d\Omega}{\int\int_\Omega T_\Omega^{-1/2} d\Omega}. \tag{16}$$

Having the expression for the temperature at point $\mathbf{x}$ the function $I(\mathbf{x})$ can be calculated from Eq. (8)

$$n(\mathbf{x}) \sqrt{T(\mathbf{x})} = \frac{K}{I(\mathrm{x})} = \frac{K}{4\pi} \int\int_\Omega \frac{d\Omega}{\sqrt{T(\mathbf{x})}}$$

$$\times \left[\frac{\int\int_\Omega T_\Omega^{1/2} d\Omega}{\int\int_\Omega T_\Omega^{-1/2} d\Omega} \right]^{\frac{1}{2}}, \tag{17}$$

which simplifies to

$$I(\mathbf{x}) = 4\pi \left[\int\int_\Omega T_\Omega^{-1/2} d\Omega \times \int\int_\Omega T_\Omega^{1/2} d\Omega \right]^{-\frac{1}{2}}. \tag{18}$$

III. KNUDSEN FORCE

We now proceed to calculate the force exerted by the gas on the cantilever and the resulting static deflection. Referring to Fig. 3, and utilizing Eq. (8) we write for the regions $\mathbf{x}_1$ far away from the cantilever, $\mathbf{x}_2$ between the cantilever and the substrate, and $\mathbf{x}_3$ immediately above the cantilever

$$\frac{P(\mathbf{x}_1) I(\mathbf{x}_1)}{\sqrt{T(\mathbf{x}_1)}} = \frac{P(\mathbf{x}_2) I(\mathbf{x}_2)}{\sqrt{T(\mathbf{x}_2)}} = \frac{P(\mathbf{x}_3) I(\mathbf{x}_3)}{\sqrt{T(\mathbf{x}_3)}}. \tag{19}$$

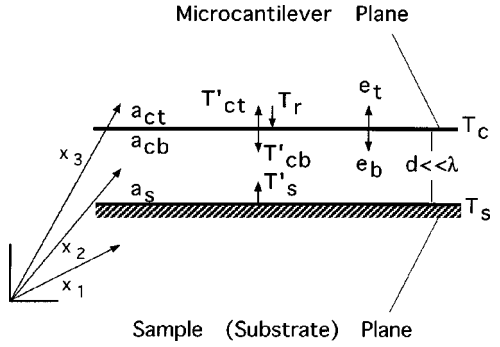

FIG. 3. The flow system composed of the microcantilever and the sample/substrate planes held at temperatures T_c and T_s, respectively, and separated by a distance d smaller than the mean-free-path λ of the molecules m. The vectors $\mathbf{x}_i$ represent the isotropic region $i=1$ away from the temperature gradient, the region between the planes $i=2$, and the region immediately above the cantilever $i=3$.

Now, the pressure at points just below and and just above the cantilever can be calculated from this invariance in terms of the pressure, temperature, and isotropicity at an arbitrary point x_1 in the system resulting in

$$P(\mathbf{x}_2)=\frac{I(\mathbf{x}_1)}{I(\mathbf{x}_2)}\sqrt{\frac{T(\mathbf{x}_2)}{T(\mathbf{x}_1)}}P(\mathbf{x}_1),$$

$$P(\mathbf{x}_3)=\frac{I(\mathbf{x}_1)}{I(\mathbf{x}_3)}\sqrt{\frac{T(\mathbf{x}_3)}{T(\mathbf{x}_1)}}P(\mathbf{x}_1). \tag{20}$$

The total force on the cantilever can then be calculated from

$$\mathbf{F}=\oint P\,\mathbf{d}S$$

$$=[P(\mathbf{x}_2)\mathbf{e}_b+P(\mathbf{x}_3)\mathbf{e}_t]\Delta S, \tag{21}$$

where $\mathbf{e}_b$, and $\mathbf{e}_t$ are unit vectors normal to the bottom and top parts of the cantilever as in Fig. 3.

In order to evaluate the quantities in Eq. (20) as given by Eqs. (16) and (18), the following energy transfer consideration introduced by Knudsen is utilized. From a balancing of energy fluxes in a diffuse scattering between two parallel plates, Knudsen calculated the heat conduction of the plates with different accommodation coefficients by introducing two opposite moving streams of molecules.[6,5] Introducing two noninteracting streams T'_s and T'_{cb} as shown in Fig. 3 in the region between the cantilever and the substrate to represent the temperatures of the molecules emerging from the substrate and the bottom surface of the cantilever with the respective accommodation coefficient a_s and a_{cb} we get

$$T'_s=\frac{a_sT_s+a_{cb}(1-a_s)T_c}{a_s+a_{cb}-a_sa_{cb}},$$

$$T'_{cb}=\frac{a_{cb}T_c+a_s(1-a_{cb})T_s}{a_s+a_{cb}-a_sa_{cb}}. \tag{22}$$

Similarly, noting that in the region above the cantilever the oncoming stream has the same temperature as that of the residual gas T_r as shown in Fig. 3, we have

$$T'_{ct}=a_{ct}T_c+(1-a_{ct})T_r. \tag{23}$$

For the two opposite moving streams represented by temperatures T'_s and T'_{cb} in the region between the cantilever and the substrate at point $\mathbf{x}_2$, the temperature $T(\mathbf{x}_2)$, and the isotropicity $I(\mathbf{x}_2)$ can also be calculated from Eqs. (16) and (18), respectively, by considering that

$$\int\int_\Omega T_\Omega^{1/2}d\Omega=\int_0^{2\pi}T_\varphi^{1/2}\int_0^{\pi}\sin\theta\,d\theta\,d\varphi$$

$$=2\int_0^{2\pi}T_\varphi^{1/2}d\varphi$$

$$=2\left(\int_0^{\pi}T_\varphi^{1/2}d\varphi+\int_\pi^{2\pi}T_\varphi^{1/2}d\varphi\right) \tag{24}$$

$$=2\left(\sqrt{T'_s}\int_0^{\pi}d\varphi+\sqrt{T'_{bc}}\int_\pi^{2\pi}d\varphi\right)$$

$$=2\pi(\sqrt{T'_s}+\sqrt{T'_{bc}}),$$

and similarly

$$\int\int_\Omega T_\Omega^{-1/2}d\Omega=2\pi\left(\frac{1}{\sqrt{T'_s}}+\frac{1}{\sqrt{T'_{bc}}}\right), \tag{25}$$

and thus Eqs. (16) and (18) are given by

$$T(\mathbf{x}_2)=\sqrt{T'_sT'_{cb}},$$

$$I(\mathbf{x}_2)=\frac{2(T'_sT'_{cb})^{1/4}}{\sqrt{T'_s}+\sqrt{T'_{cb}}}. \tag{26}$$

As mentioned, in the region above the cantilever at $\mathbf{x}=\mathbf{x}_3$, the oncoming stream (from the upper half space) originates from the isotropic region with a temperature T_r and thus an integration similar to Eq. (24) results in

$$T(\mathbf{x}_3)=\sqrt{T_rT'_{ct}},$$

$$I(\mathbf{x}_3)=\frac{2(T_rT'_{ct})^{1/4}}{\sqrt{T_r}+\sqrt{T'_{ct}}}. \tag{27}$$

Finally, in the region far away from the cantilever and the substrate at $\mathbf{x}=\mathbf{x}_1$, the streams in the upper and lower half spaces have the same temperature which results in

$$T(\mathbf{x}_1)=\sqrt{T_rT_r}=T_r,$$

$$I(\mathbf{x}_1)=\frac{2(T_rT_r)^{1/4}}{\sqrt{T_r}+\sqrt{T_r}}=1. \tag{28}$$

Thus, using Eq. (20) in Eq. (21) along with Eq. (28), the force per unit area from Eq. (21) is given by

$$F=P_r\left[\frac{1}{I(\mathbf{x}_2)}\sqrt{\frac{T(\mathbf{x}_2)}{T_r}}-\frac{1}{I(\mathbf{x}_3)}\sqrt{\frac{T(\mathbf{x}_3)}{T_r}}\right], \tag{29}$$

or using Eqs. (26) and (27) and simplifying

$$F=\frac{P_r}{2}\left[\sqrt{\frac{T'_s}{T_r}}+\sqrt{\frac{T'_{cb}}{T_r}}+\sqrt{\frac{T'_{ct}}{T_r}}-1\right]. \tag{30}$$

Therefore, using Eqs. (22) and (23) in Eq. (30) the force per unit area for known accommodation coefficients a_i of the two sides of the cantilever and the surface of the substrate can be written as

$$F(T_s, T_c, T_0, P_r) = g(T_s, T_c, T_r) P_r, \tag{31}$$

where the dimensionless function g is given by

$$g(T_s, T_c, T_r) = \frac{1}{2}\left[\sqrt{\frac{a_s \tau_s + a_{cb}(1-a_s)\tau_c}{a_s + a_{cb} - a_s a_{cb}}} + \sqrt{\frac{a_{cb}\tau_c + a_s(1-a_{cb})\tau_s}{a_s + a_{cb} - a_s a_{cb}}} + \sqrt{1 - a_{ct} + a_{ct}\tau_c} - 1 \right], \tag{32}$$

where $\tau_s = T_s/T_r$ and $\tau_c = T_c/T_r$. Thus, for fixed (a_i, T_i) with i spanning the substrate, cantilever, and the rest gas, the function $g(T_s, T_c, T_0) = \alpha$ is a constant, and the force varies linearly with the pressure in the rarefied regime, that is so long as P_r is such that $\mathrm{Kn}(P_r) > \mathrm{Kn}(P_{rm})$ where P_{rm} is a maximum pressure beyond which the effect of intermolecular collisions will be non-negligible in the surface–gas and gas–surface energy transport. Then with the constant given by

$$\alpha = \left(\frac{\partial F}{\partial P_r} \right)_{T_s, T_c, T_r}, \tag{33}$$

any variation in (a_i, T_i) only changes the slope of the line $F(P_r) = \alpha P_r$. It can be easily shown from Eq. (31) by setting $\tau_s = 1$ or $\tau_c = 1$ in Eq. (32) that all the limiting cases $a_{cb} = a_{ct} \neq a_s$; and $a_s = a_{cb} = a_{ct} = a$ with $a \neq 1$ and $a = 1$ reduce correctly to the results found in Refs. 6 and 35. In particular, for the case of an isolated cantilever, the form of g can be obtained by assuming that the stream emerging from the substrate belongs to the same class of velocities as the stream moving toward the top of the cantilever (see Fig. 3), i.e., $T_s' , T_s \to T_r$. It can then be seen from Eq. (22) that $a_s = 1$, and from Eq. (30) that g must be given by

$$g(T_c, T_r) = \frac{1}{2}\left[\sqrt{1 - a_{cb} + a_{cb}\tau_c} - \sqrt{1 - a_{ct} + a_{ct}\tau_c} \right], \tag{34}$$

which, as mentioned in Sec. II, will go to zero if either $a_{cb} \to a_{ct}$ or $T_c \to T_r$.

Finally, having the force, we proceed to calculate the deflection of the cantilever. The transverse vibrations of a cantilever exposed to an arbitrary resistive force $R(x, t)$, and an arbitrary driving force $F(x, t)$ can be described by[38]

$$EI \frac{\partial^4 W(x,t)}{\partial x^4} + \mu \frac{\partial^2 W(x,t)}{\partial t^2} + R(x,t) = F(x,t), \tag{35}$$

subject to the standard fixed-free beam boundary conditions

$$W(0,t) = W_x(0,t) = W_{xx}(L,t) = W_{xxx}(L,t) = 0, \tag{36}$$

and the initial condition $W(x, t_0) = 0$, where the positive constants E, I, and μ are Young's modulus, area moment of inertia, and the mass per unit length, respectively. Using these definitions, it is then understood that $R(x, t)$, and $F(x, t)$ are forces per unit length of the cantilever. Neglecting damping for an undriven cantilever of length L in the static limit, and under the influence of the uniform normal force per unit area F given in Eq. (31), Eq. (35) reduces to

$$EI \frac{d^4 W(x)}{dx^4} = F\Theta(L - x), \tag{37}$$

where Θ is the Heaviside function. It is noted here that for cantilevers of arbitrary shape and no particular relation between length and width, one must solve the full plate equation for the static deflection $W(x, y)$.[39] However, in our case, the length of the cantilever is assumed to be much larger than the width, as in most AFM work, and thus Eq. (37) is justified, that is $W(x, y) \approx W(x)$. We now proceed by integrating Eq. (37) twice from $x \to L$ and twice from $0 \to x$ and utilizing Eqs. (36) and (31) to yield

$$W(x, T_s, T_c, T_r, P_r) = \frac{P_r}{EI}\left(\frac{1}{24}x^4 - \frac{L}{6}x^3 + \frac{L^2}{4}x^2 \right) \times g(T_s, T_c, T_r), \tag{38}$$

or in terms of the maximum deflection $W_{\max}$ of the cantilever for given T_s, T_c, T_r, and P_r

$$W(x) = \frac{W_{\max}}{3}\left[\left(\frac{x}{L}\right)^4 - 4\left(\frac{x}{L}\right)^3 + 6\left(\frac{x}{L}\right)^2 \right]. \tag{39}$$

IV. RESULTS AND DISCUSSIONS

The radiation effects are assumed negligible in the heat conduction process considered here. The contribution of radiation to the heat transfer between the cantilever and the sample can be estimated assuming that the emissivity ε of the cantilever material (silicon nitrite), and sample material, is known. For the cantilever and sample in thermal equilibrium with the residual gas, the net radiation exchange is obviously zero. Therefore, assuming that the rest gas is transparent to radiation, increasing the cantilever temperature to $T_c > T_s = T_r$, results in a net exchange of $q = \sigma l_x l_y (T_c^4 - T_r^4)\mathcal{F}_{cs}[\mathrm{W\,m^{-2}K^{-4}}]$ in the black-body limit, where σ is the Stefan–Boltzmann constant, and $\mathcal{F}_{cs}$ is the configuration factor which only depends on the geometry. Modeling the sample surface with a disk of radius $R \gg l_x$ facing the cantilever which is located at a distance $d = 10.0\,\mu\mathrm{m}$ above it, it can be shown that $\mathcal{F}_{cs} = 1/[1 + (d/R)^2] \approx 1$. Therefore, the ratio γ of the radiation delivered diffusely by the cantilever to the sample surface to that delivered diffusely by the upper half space of the vacuum system can be shown to be of the order $\gamma \approx \varepsilon_{cs} A_{cs} \tau_c^4$, where ε_{cs}, and A_{cs} are the ratios of the cantilever to sample emissivities and the areas, respectively. In the black body limit $\varepsilon_{cs} \to 1$, this would correspond to $\gamma = 1.2 \times 10^{-4}$.

We also note here that optical heating of the cantilever via a laser beam results typically in a focused illumination spot along the cantilever and, thus, the temperature is raised initially in that region giving the cantilever a temperature gradient along its physical length. Existence of such a gradient could then result in slip flow for a certain region of

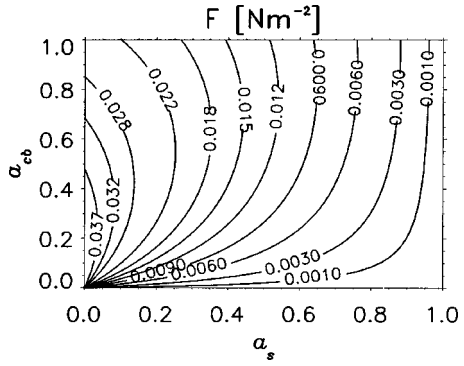

FIG. 4. Force per unit area for $a_{ct}=a_{cb}$, acting on the cantilever held at a temperature $T_c=330$ K, while the sample and the rest gas are at $T_s=T_r=300$ K with $P_r=10.0$ μbar.

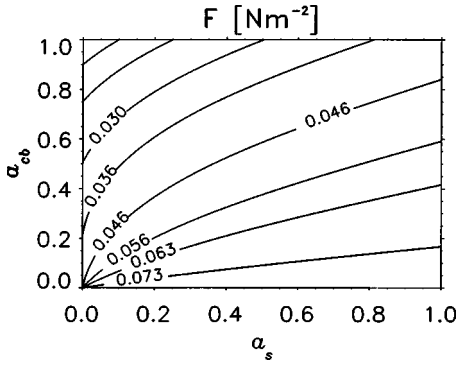

FIG. 5. Force per unit area for $a_{ct}=a_{cb}$, acting on the cantilever held at a temperature $T_c=325$ K, while the sample temperature is raised to $T_s=350$ K above the rest gas temperature $T_r=300$ K with $P_r=10.0$ μbar.

Knudsen number. Here, it has been assumed that no such gradient is present and the cantilever is uniformly heated.

The extension of the microcantilever–substrate assembly to Lockenvitz model[34] for the vacuum gauge application or to an array of cantilevers juxtaposed with surfaces at various temperatures is straightforward. Each cantilever (placed between two parallel surfaces similar to that proposed by Lockenvitz) at temperature T_i in such an arrangement would then deflect according to an equation similar to Eq. (38), and the pressure P_i could be extracted from $W^i_{\max}$, so that the pressure of the system would be $P\propto\Sigma_i W^i_{\max}/i$. These considerations are currently being investigated experimentally by the authors in order to examine the sensitivity and accuracy of such an arrangement as a potential vacuum gauge.

The results presented here are for a pressure $P_r=10.0$ μbar. In lieu of Eq. (38), for the same temperature ratios τ_c, and τ_s, the results at other pressures $P_r=10.0\times\beta$ μbar can be achieved by multiplying the presented results by β subject to $P_r<P_{rm}$. Using Eqs. (31) and (38), we can estimate the Knudsen forces on commercially available AFM cantilevers and their subsequent deflections. In doing so, we will treat the energy accommodation coefficients a_i as parameters due to the lack of measured material data. We first note that if the fundamental vacuum frequency ω_1 of the cantilever is known, the parameters representing the elastic properties of the cantilever can be removed from Eq. (35) by the substitution

$$\omega_1=\left(\frac{\lambda_1}{L}\right)^2\left(\frac{EI}{\mu}\right)^{\frac{1}{2}}, \tag{40}$$

where $\lambda_1=1.875$ is the smallest positive root of equation $1+\cos\lambda_n\cosh\lambda_n=0$. However, assuming a rectangular cantilever of dimensions $\ell_x=200$ μm length, $\ell_y=20$ μm width, and $\ell_z=0.6$ μm thickness made of silicon with a mass density of $\rho=2.33$ g/cm^3 and Young modulus $E=1.79\times10^{11}$ Pa, the area moment of inertia can be calculated to be $I=\ell_y\ell_z^3/12=3.6\times10^{-25}$ m^4. Incidentally, this corresponds to a mass per unit length of $\mu=\rho\ell_z\ell_y=3.0\times10^{-8}$ and thus a fundamental vacuum frequency Eq. (40) of $\omega_1=133.43$ kHz.

Figure 4 displays in units of Nm^{-2}, and as a function of the accommodation coefficients a_{cb}, and a_s, the uniform force per unit area for the case $a_{ct}=a_{cb}$ with a temperature distribution of $T_c=330$ K, $T_s=T_r=300$ K.

For the same selection of the accommodation coefficients, the force behaves differently while still in the same direction as before when the sample temperature $T_s=350$ K is higher than that of the cantilever $T_c=325$ K, and the rest gas $T_r=300$ K as shown in Fig. 5.

For the cantilever dimensions just specified, and noting that the force in Eq. (31) is in units of N/m^2, whereas in Eq. (37) it is in N/m, Fig. 6 displays the cantilever deflection in units of nm, and as a function of the accommodation coefficients for the bottom and top surfaces of an isolated cantilever held at temperature $T_c=330.0$ K. As can be seen in Fig. 6, the deflection changes direction depending on whether the point (a_{cb}, a_{ct}) lies to the right- or left-hand side of the line $a_{cb}=a_{ct}$ along which the net force is zero. Also, for the same point in the accommodation plane, the force and thus the deflection reverses direction depending on whether the cantilever is heated $\tau_c>1$ or cooled $\tau_c<1$. This can be seen clearly, for example, for the point $(a_{cb}, a_{ct})=(0.9, 0.6)$ in Fig. 7 at $\tau_c=1.0$.

V. CONCLUSIONS

The results presented here can be used to estimate the temperature and pressure ranges where the Knudsen forces become important in microcantilever applications. Similarly,

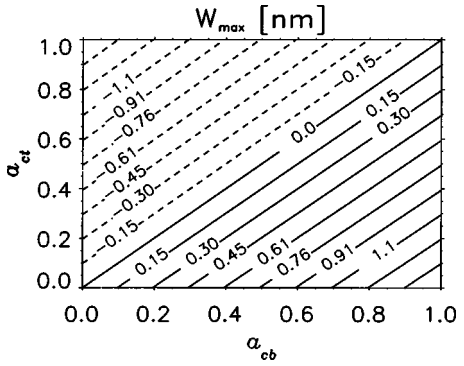

FIG. 6. Maximum deflection of an isolated cantilever held at $T_c=330$ K in the free molecular regime at $P_r=10.0$ μbar, and $T_r=300$ K.

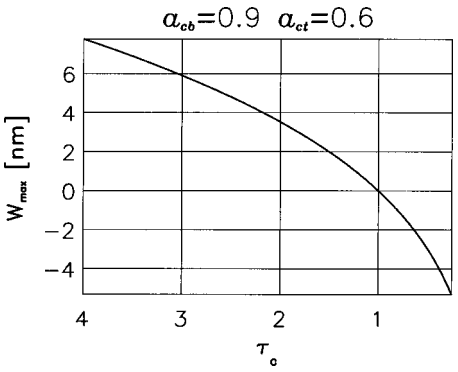

FIG. 7. Maximum deflection of an isolated cantilever as a function of the relative temperature of the cantilever and the residual gas τ_c in the free molecular regime at $P_r = 10.0\ \mu$bar.

for given temperature distributions and pressure, the magnitude of the deflection can be estimated using these results. These estimates are important in many cases since, in general, in order to incorporate the geometrical characteristics, such as shape dependency and surface roughness of the cantilever/sample, one has to resort to multidimensional numerical methods such as DSMC. Based on these estimates, the potential of the application of a microcantilever assembly to vacuum measurements was proposed.

ACKNOWLEDGMENTS

This work was supported by the U.S. DOE Office of Biological and Environmental Research (OBER). Oak Ridge National Laboratory, Oak Ridge, TN, 37831-6123, is managed by UT-Battelle, LLC for the Department of Energy under Contract No. DE-AC05-0096OR22725.

APPENDIX

$$\int_0^\infty x^2 e^{-\beta^2 x^2} dx = \frac{\sqrt{\pi}}{4\beta^3}, \tag{A1}$$

$$\int_0^\infty x^4 e^{-\beta^2 x^2} dx = \frac{\sqrt{3\pi}}{8\beta^5}. \tag{A2}$$

[1] B. C. Moore, J. Vac. Sci. Technol. **1**, 10 (1964).
[2] B. C. Moore, J. Vac. Sci. Technol. **6**, 246 (1969).
[3] J. M. Lafferty, *Foundations of Vacuum Science and Technology* (Wiley, New York, 1998).
[4] T. A. Delchar, *Vacuum Physics and Techniques* (Chapman and Hall, London, 1993).
[5] E. H. Kennard, *Kinetic Theory of Gases* (McGraw–Hill, New York, 1938).
[6] M. Knudsen, *The Kinetic Theory of Gases* (Methuen, London, 1950).
[7] E. A. Mason and A. P. Malinauskas, Oak Ridge National Laboratory Report, ORNL-3796, (1965).
[8] Y. Wu, J. Chem. Phys. **48**, 889 (1968).
[9] J. M. Laffert, in *Vacuum Techniques*, edited by S. Dushman and J. M. Laffert (1962).
[10] J. M. Thomas and J. A. Poulis, in *Vacuum Microbalance Techniques*, edited by K.H. Behrndt (Plenum, New York, 1963).
[11] E. Robens, *Vacuum Microbalance Techniques*, (Plenum, New York, 1971), Vol. 8.
[12] J. L. Garcia Fierro and A. M. Alvarez Garcia, Vacuum **31**, 79 (1981).
[13] S. C. Linag, J. Appl. Phys. **22**, 148 (1951).
[14] S. C. Liang, J. Phys. Chem. **56**, 660 (1952).
[15] S. 4C. Liang, J. Phys. Chem. **57**, 910 (1953).
[16] S. C. Liang, Can. J. Phys. Chem. **33**, 279 (1955).
[17] T. Takaishi and Y. Sensui, Trans. Faraday Soc. **59**, 2503 (1963).
[18] D. C. York, A. Chambers, and A. P. Troup, Vacuum **59**, 910 (2000).
[19] D. C. York, A. Chambers, A. D. Chew, and A. P. Troup, Vacuum **55**, 133 (1999).
[20] B. K. Annis, J. Chem. Phys. **57**, 2898 (1972).
[21] S. K. Loyalka, J. Chem. Phys. **55**, 4497 (1971).
[22] S. K. Loyalka, J. Chem. Phys. **66**, 4935 (1977).
[23] C. Cercignani, *Rarefied Gas Dynamics* (Cambridge University Press, Cambridge, UK, 2000).
[24] Y. Wu, J. Plasma Phys. **1**, 209 (1967).
[25] Y. Wu, in *Rarefied Gas Dynamics*, edited by L. Talbot (Academic, New York, 1961), Suppl. 1, p. 141.
[26] Y. Wu, in *Rarefied Gas Dynamics*, edited by J. H. de Leeuw (Academic, New York, 1965), Suppl. 3, p. 677.
[27] K. Aoki, Y. Sone, and Y. Waniguchi, Comput. Math. Appl. **35**, 15 (1998).
[28] T. Ohwada, Y. Sone, and K. Aoki, Phys. Fluids A **1**, 2042 (1989).
[29] T. Ohwada, Y. Sone, and K. Aoki, Phys. Fluids A **1**, 1588 (1989).
[30] Y. Sone, T. Ohwada, and K. Aoki, Phys. Fluids A **1**, 363 (1989).
[31] Y. Wu, J. Chem. Phys. **47**, 2617 (1967).
[32] H. E. Marsh, E. Condon, and L. B. Loeb, J. opt. Soc. Am. **11**, 257 (1925).
[33] Y. Wu, Ann. Physik **7**, 144 (1967).
[34] A. E. Lockenvitz, Rev. Sci. Instrum. **9**, 417 (1938).
[35] Y. Wu, Ann. Physik **7**, 21 (1966).
[36] Y. Wu, J. Vac. Sci. Technol. **9**, 1248 (1972).
[37] J. P. Hobson and D. B. Salzman, J. Vac. Sci. Technol. A **18**, 1758 (2000).
[38] K. F. Graff, *Wave Motion in Elastic Solids* (Ohio State University Press, Columbus, 1975).
[39] J. E. Sader, J. Appl. Phys. **74**, 1 (1993).